

1 **Bioinformatics analysis identifies potential ferroptosis-related key genes in the**  
2 **pathogenesis of diabetic nephropathy**

3  
4 Shiqiang Zhao, Fu Zheng\*

5  
6 Nephrology Department, Sir Run Run Shaw Hospital, Zhejiang University School of  
7 Medicine, Hangzhou, 311399, China

8  
9 **\*Corresponding author**

10 Fu Zheng: 1060271325@qq.com

11  
12 **Abstract**

13 **Objective:** To identify potential ferroptosis-related key genes in the pathogenesis of  
14 diabetic nephropathy (DN) through bioinformatics analysis, thereby providing new  
15 targets for the treatment of DN.

16 **Methods:** We first downloaded the RNA expression dataset GSE30529 from the GEO  
17 database and intersected it with a ferroptosis dataset to obtain ferroptosis-related  
18 differentially expressed genes (DEGs). Venny 2.1 was used to generate Venn diagrams  
19 of the DEGs, and Heml software was used to draw heatmaps of the DEGs. DAVID  
20 6.8, Metascape, and WebGestalt were employed for functional enrichment analysis of  
21 the DEGs. Protein-protein interactions (PPIs) were retrieved through the STRING  
22 database and visualized by Cytoscape v3.6.0 software. miRWalk 2.0 was used to  
23 predict target key miRNAs and construct related gene-miRNA interaction networks.

24 **Results:**

25 Our study identified 31 ferroptosis-related DEGs. Gene Set Enrichment Analysis  
26 (GSEA) revealed that the biological processes of these genes were significantly  
27 enriched in response to stress signals, starvation signals, lipids and atherosclerosis,  
28 and regulation of endogenous apoptotic signaling pathways, among others. The  
29 regulatory network of the MAPK8 molecule is the most crucial potential molecule

30 that may affect the occurrence of DN. The endogenous apoptotic signaling pathway is  
31 the main biological pathway involved. We screened out one key module through  
32 MCODE, which includes two downregulated genes (MAPK8 and DDIT3) and three  
33 upregulated genes (XBP1, HSPA5, and ASNS).

#### 34 **Conclusion:**

35 The ferroptosis-related key genes MAPK8, has-miR-4775, HSPA5, has-miR-4712-  
36 5p/has-miR-770-5p, and XBP1 form a regulatory network, participating in the  
37 occurrence and development of DN. This provides some important references for our  
38 future basic research verification and suggests a potential target for the development  
39 of DN treatment strategies.

40 **Keywords:** Diabetic Nephropathy; Ferroptosis; MAPK8; Bioinformatics Analysis;  
41 Target

#### 42 **1. Introduction**

43 Diabetic Nephropathy (DN) is one of the most common microvascular complications  
44 of diabetes [1] and a major cause of end-stage renal disease (ESRD), which is  
45 associated with inflammation and immune responses [2-3]. DN is a significant public  
46 health issue worldwide. According to statistics, there are approximately 420 million  
47 diabetics globally, with one in every four women and one in every five men having  
48 type 2 diabetes and diabetic nephropathy, a phenomenon more common in type 1  
49 diabetes [4]. From a pathophysiological perspective, DN can be divided into  
50 glomerular lesions, tubular and interstitial atrophy and fibrosis. Its clinical features  
51 include a continuous decline in glomerular filtration rate, accompanied by persistent  
52 elevations in proteinuria and serum creatinine [5]. After the occurrence of DN, many  
53 factors are triggered, among which the reduction of renal tissues or cells that can play  
54 an active and effective role is the main factor leading to the reduction of renal  
55 function.

56 Previous studies have also shown that programmed cell death plays an important role  
57 in the development of DN [6-7]. Ferroptosis is a programmed cell death-like process  
58 characterized by the production and accumulation of iron-dependent lipid reactive

59 oxygen species (ROS) [8]. Studies have reported that ferroptosis plays an important  
60 role in the occurrence and development of many diseases, such as targeting iNOS to  
61 reduce early brain injury after experimental subarachnoid hemorrhage by promoting  
62 ferroptosis of M1 microglia and reducing neuroinflammation [9]; the loss of heart  
63 ferritin H promotes cardiomyopathy through Slc7a11-mediated ferroptosis [10]; and  
64 the loss of iron transporter proteins induces memory impairment by promoting  
65 ferroptosis in Alzheimer's disease [11]. However, the mechanism of ferroptosis in DN  
66 is still unclear, and there is also a lack of related bioinformatics research. We used  
67 data mining and data analysis techniques to screen for differentially expressed genes  
68 (DEGs) in diseased renal tissues and normal renal tissues of DN. These DEGs were  
69 then intersected with the ferroptosis dataset to obtain ferroptosis-related DEGs.  
70 In addition, to identify key biomarkers and establish the pathogenesis of DN at the  
71 molecular level, we investigated key miRNAs that may play a major role in DN. Our  
72 research results will help to understand the state of ferroptosis after the occurrence of  
73 DN and provide new ideas for the clinical diagnosis and treatment of DN.

## 74 **2. Materials and Methods**

### 75 **2.1 GEO Data Analysis**

76 The RNA expression dataset GSE30529 (containing diseased renal tissues and normal  
77 renal tissues of DN) was downloaded from the GEO database  
78 (<https://www.ncbi.nlm.nih.gov/geo/query/acc.cgi>) using the GEOquery package.  
79 Probes corresponding to multiple molecules were removed, and when probes  
80 corresponding to the same molecule were encountered, only the probe with the largest  
81 signal value was retained.

### 82 **2.2 Ferroptosis Data Analysis**

83 Relevant ferroptosis datasets were downloaded from the ferroptosis database  
84 (<http://www.zhounan.org/ferrdb>), which contains 259 genes. The annotations of these  
85 genes reveal 108 driver genes, 69 inhibitory genes, and 111 gene markers [12].

### 86 **2.3 Differential Expression Analysis**

87 GEO2R is an online tool for differential expression analysis [13]. The T-test was used

88 to determine p-values and adjusted p-values in differential gene expression (DGE)  
89 analysis. Genes from different tissues were selected using the following criteria:  
90  $|\log_2(\text{fold-change})| > 1$ , adjusted p-value  $< 0.05$ . We also obtained a dataset that  
91 included genes from the ferroptosis database and intersected it with GSE30529 to  
92 identify ferroptosis-related DEGs. The online tool Venny 2.1 was used to generate  
93 Venn diagrams of the DEGs, and Heml software was used to draw heatmaps of the  
94 DEGs.

#### 95 **2.4 Functional Enrichment Analysis**

96 DAVID 6.8, Metascape, and WebGestalt were used for functional enrichment analysis  
97 of the DEGs. These different enrichment analysis tools have different algorithms,  
98 which can serve as mutual validation. We uploaded the ferroptosis-related DEGs to  
99 WebGestalt's GSEA for further study. WebGestalt's GSEA first filters gene sets based  
100 on the number of genes they contain. KEGG analysis was obtained from WebGestalt's  
101 GSEA. Metascape is an online tool for gene function annotation analysis. The  
102 biological process annotations were performed by Metascape using genes shared  
103 between GSE30529 and the ferroptosis dataset. Additionally, the biological pathways  
104 of miRNAs were analyzed in the enrichment analysis tool Funrich. A p-value  $< 0.05$   
105 was considered statistically significant.

#### 106 **2.5 Protein-Protein Interaction Network Analysis**

107 To predict protein-protein interactions (PPIs), we searched for interactions between  
108 these proteins through the STRING database. Furthermore, the PPI network was  
109 constructed and visualized by Cytoscape v3.6.0 software. Molecular Complex  
110 Detection (MCODE) was used for clustering analysis of the gene network to identify  
111 key PPI network modules. The function of MCODE is to select key subnetworks, i.e.,  
112 modules. A PPI module refers to a PPI that serves a single function. In a module,  
113 different genes have different module scores, and key genes can be selected based on  
114 the scores. To identify key modules, a p-value  $< 0.05$  was considered to indicate  
115 significant differences.

#### 116 **2.6 Gene-miRNA Interaction Network**

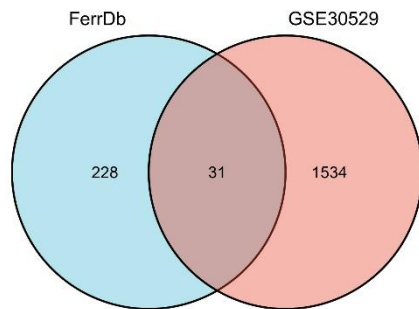
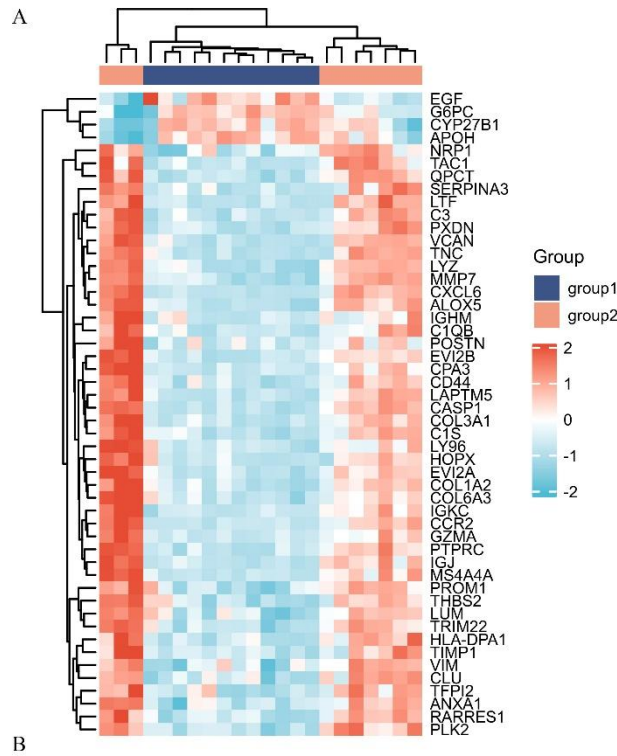
117 We used miRWalk 2.0 to predict target key miRNAs and construct related gene-  
118 miRNA interaction networks. We intersected the prediction results from the  
119 MiRTarBase and miRWalk databases to ensure the accuracy of our results. We  
120 screened for miRNAs that target more than two genes.

## 121 **2.7 Statistical Analysis**

122 GraphPad Prism 7.0 software was used for graphing and statistical analysis. All data  
123 are presented as mean  $\pm$  standard deviation (SD). In DGE analysis, the t-test was used  
124 to determine p-values and adjusted p-values, where p-values were adjusted by FDR. A  
125 p-value  $< 0.05$  indicated a statistically significant difference.

## 126 **3. Results**

127 **3.1** The microarray expression profile analysis dataset GSE30529 was downloaded  
128 from the GEO database, and DEGs were obtained by comparing diseased renal tissues  
129 and normal renal tissues of DN. The heatmap and Venn diagram of the DEGs are  
130 shown in Figure 1.



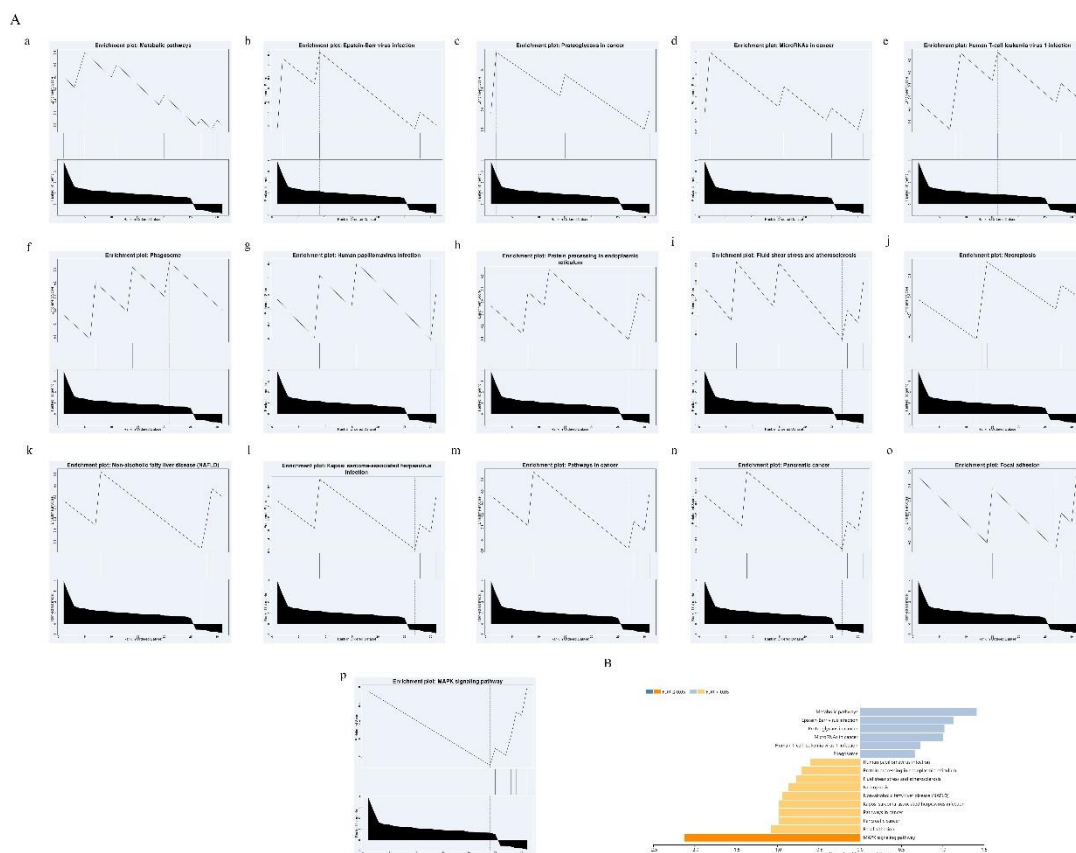
131  
 132 Figure 1. (A) There are 1565 differentially expressed genes (DEGs) in diseased renal  
 133 tissues and normal renal tissues of DN. The top 50 DEGs are shown in the heatmap,  
 134 with red representing genes significantly upregulated in the samples and blue  
 135 representing significantly downregulated genes; (B) Venn diagram of ferroptosis-  
 136 related DEGs. We intersected the ferroptosis dataset with GSE30529 to identify 31  
 137 ferroptosis-related DEGs.

138

### 139 3.2 Enrichment Pathways and Analysis of Ferroptosis-related DEGs

140 The enrichment analysis of DEGs was conducted using online tools such as  
 141 Metascape, WebGestalt, and DAVID. Firstly, we uploaded the relevant information of  
 142 DEGs from both DN-affected and normal kidney tissues containing DN to the

143 WebGestalt software. The results of the enriched gene dataset analysis indicated that  
 144 the significantly enriched genes were predominantly involved in metabolic pathways,  
 145 Epstein-Barr virus infection, proteoglycans in cancer, MAPK signaling pathway, etc.  
 146 (Figure 2). DAVID was used to analyze the biological pathways and processes of  
 147 these 31 DEGs in the samples. The KEGG functional analysis revealed that the gene  
 148 set was significantly activated in areas such as prion diseases, fluid shear stress and  
 149 atherosclerosis, spinocerebellar ataxia, pancreatic cancer, and protein processing in  
 150 endoplasmic reticulum (Figure 3). Secondly, the 31 DEGs were uploaded to  
 151 Metascape, and the results showed that the biological processes were significantly  
 152 enriched in cellular responses to stress signals, responses to starvation signals, lipids  
 153 and atherosclerosis, regulation of endogenous apoptotic signaling pathways, etc.  
 154 Moreover, the biological processes were significantly activated in response to stress  
 155 (Figure 4). Notably, the endogenous apoptotic signaling pathway was the primary  
 156 biological pathway involved.



157

158 Figure 2. The results of the enriched gene dataset analysis showed that the

159 significantly enriched genes were mainly involved in the MAPK signaling pathway.  
 160 The gene set enrichment analysis of WebGestalt first filtered the gene sets based on  
 161 the number of genes contained, with a default minimum of 7 genes and a maximum of  
 162 2000 genes.

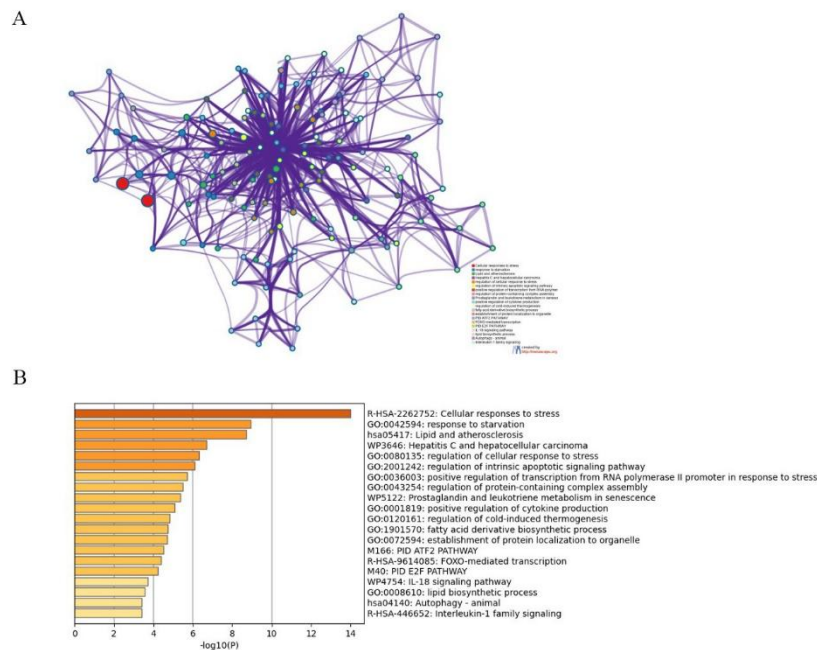
163

| ONTOLOGY | Description                                 | GeneRatio | pvalue   | qvalue |
|----------|---------------------------------------------|-----------|----------|--------|
| KEGG     | Prion disease                               | 6/27      | 2.30e-04 | 0.025  |
| KEGG     | Fluid shear stress and atherosclerosis      | 4/27      | 0.001    | 0.044  |
| KEGG     | Spinocerebellar ataxia                      | 4/27      | 0.001    | 0.044  |
| KEGG     | Pancreatic cancer                           | 3/27      | 0.002    | 0.051  |
| KEGG     | Protein processing in endoplasmic reticulum | 4/27      | 0.002    | 0.051  |

164

165 Figure 3. The pathway directions that the gene sets may participate in were selected  
 166 and displayed based on enrichment scores.

167



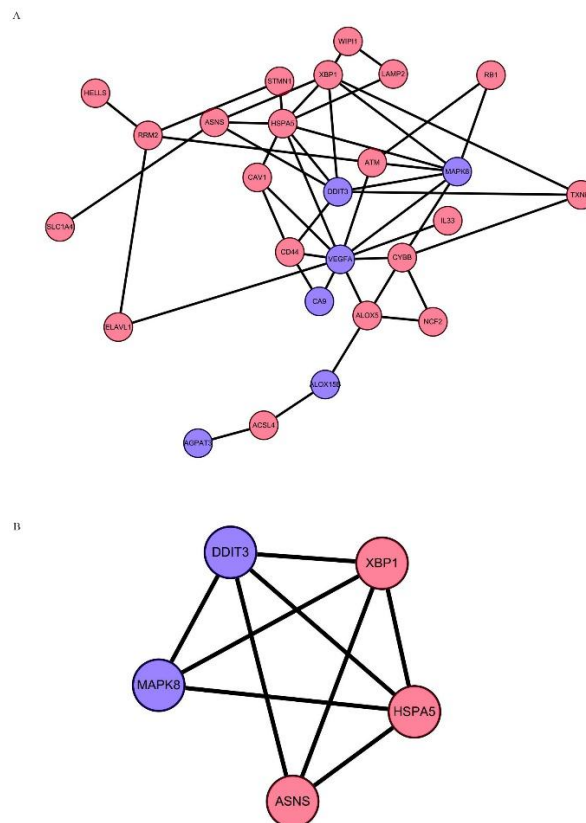
168

169 Figure 4. (A) Enrichment network. (B) Metascape plotted a bar chart of 20 biological  
 170 pathways based on P-values and gene percentages, where biological pathways with P-  
 171 values < 0.01 were statistically significant.

172

173 **3.3 Protein-Protein Interaction Network Analysis of Ferroptosis-related DEGs**

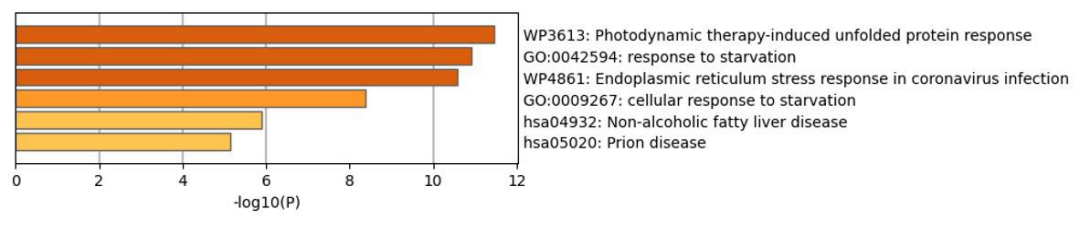
174 We obtained a network containing 26 nodes. The network was set to the default cutoff  
 175 value (interaction score > 0.4) in the STRING online database. Genes are represented  
 176 by nodes, and interactions between genes are represented by edges. Up-regulated  
 177 genes are marked in red, while down-regulated genes are marked in blue. MCODE, an  
 178 application of Cytoscape, was used for cluster analysis of the gene network to identify  
 179 key modules. One key module was established, consisting of 2 down-regulated genes  
 180 (MAPK8 and DDIT3) and 3 up-regulated genes (XBP1, HSPA5, and ASNS). These 5  
 181 genes are the key genes screened by MCODE. Additionally, functional analysis using  
 182 Metascape indicated that these 5 genes are mainly involved in protein folding  
 183 responses in photodynamic therapy-induced starvation responses, endoplasmic  
 184 reticulum stress responses in coronavirus infections, and cellular responses to  
 185 starvation (Figure 6).



186  
 187 Figure 5. (A) Cytoscape network visualization of 26 nodes obtained from the  
 188 STRING online database, with an interaction score > 0.4. Nodes represent genes, and  
 189 edges represent connections between genes. Red represents up-regulated genes, and

190 blue represents down-regulated genes. (B) MCODE identified one key module for  
191 identifying gene clusters in the network.

192



193

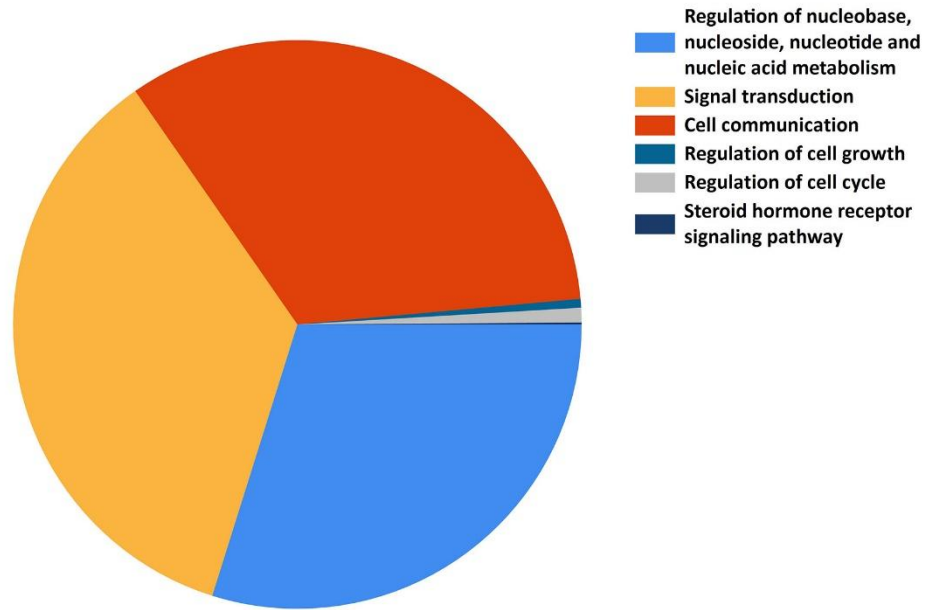
194 Figure 6. Functional enrichment analysis.

### 195 3.4 Further miRNA Interaction and Exploration

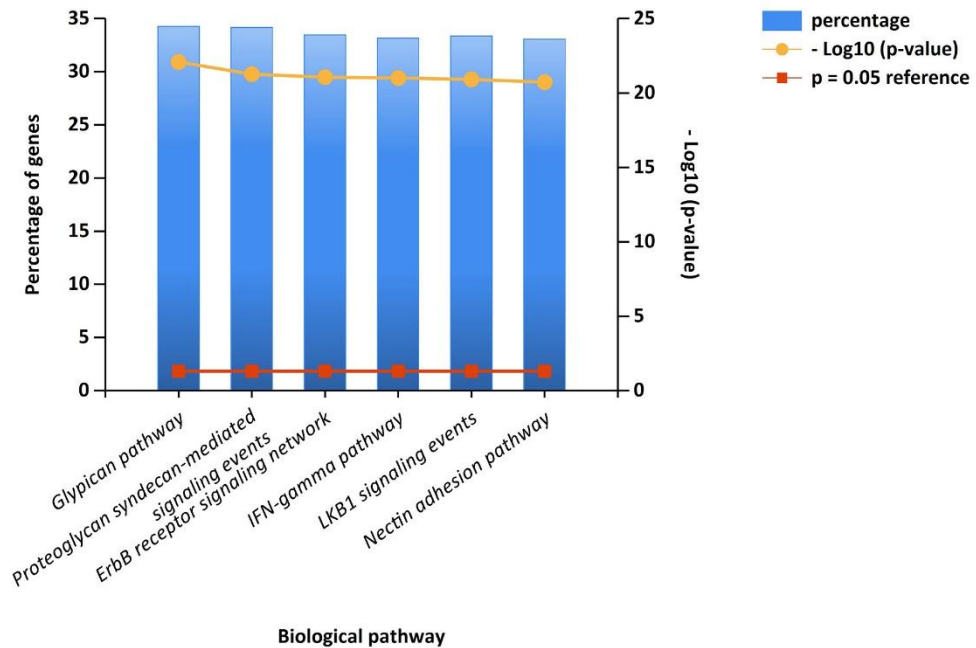
196 We screened the 5 genes in the previous key module and conducted gene-miRNA  
197 analysis using miRWalk 2.0 software. The cross-linked miRNAs were selected from  
198 the miRWalk and miRTarBase databases to ensure the accuracy and reliability of our  
199 results. The following criteria were used to filter the results:  $p < 0.05$ , seed sequence  
200 length  $> 7$ , and 3'UTR as the target gene binding region. Therefore, we speculate that  
201 the ferroptosis-related key genes MAPK8, has-miR-4775, HSPA5, has-miR-4712-  
202 5p/has-miR-770-5p, and XBP1 form a regulatory network, thereby participating in the  
203 occurrence and development of diabetic nephropathy (Figure 7). The enrichment  
204 analysis results showed that their molecular functions were significantly enriched in  
205 the regulation of nucleobase, nucleotide, and nucleic acid metabolism, and cellular  
206 signal transduction. The enriched biological pathways include proteoglycan synthesis-  
207 mediated signaling events, ErbB receptor signaling network, and IFN- $\gamma$  signaling  
208 pathway (Figure 8).



A



B



213

214 Figure 8. (A) The molecular functions of miRNAs targeting genes in the key module  
 215 were significantly enriched in the regulation of nucleobase, nucleotide, and nucleic  
 216 acid metabolism, and cellular signal transduction. (B) Biological pathways were  
 217 enriched in proteoglycan synthesis-mediated signaling events, ErbB receptor  
 218 signaling network, and IFN- $\gamma$  signaling pathway.

219

220 **4 Discussion**

221 This study identified key genes involved in ferroptosis and further explored the  
222 possible mechanisms related to ferroptosis in DN. Our study obtained 31 DEGs from  
223 the intersection of dataset GSE30529 and ferroptosis-related DEGs. Then, we used  
224 online tools such as Metascape, GSEA, and DAVID to conduct GSEA enrichment  
225 analysis of DEGs. The results showed that the biological processes of these genes  
226 were significantly enriched in cellular responses to stress signals, responses to  
227 starvation signals, lipids and atherosclerosis (free radicals, etc.), and regulation of  
228 endogenous apoptotic signaling pathways. Moreover, these biological processes were  
229 significantly activated in response to stress. Additionally, the regulatory network of  
230 the MAPK8 molecule may affect signaling pathway changes in DN. The study also  
231 identified several genes that have not been mentioned in the field of DN and  
232 ferroptosis. This study can provide an effective reference for the pathological  
233 mechanism of DN from the perspective of bioinformatics analysis.

234 Ferroptosis is characterized by the intracellular accumulation of lipid ROS, which are  
235 closely related and ultimately lead to lipid oxidation, causing cell membrane damage  
236 and cell death. Ferroptosis is associated with oxidative stress generated by excessive  
237 accumulation of ROS during aerobic metabolism [14]. After oxidative stress, some  
238 signaling pathways are activated, such as the MAPK pathway. According to previous  
239 studies, the MAPK pathway may induce the production of free radicals after DN,  
240 which can induce ferroptosis and apoptosis [15-16]. In this context, antioxidant  
241 therapy may reduce apoptosis after the occurrence of DN. A previous study showed  
242 that the MAPK pathway is activated after iron accumulation, and inhibiting MAPK  
243 activation can improve functional outcomes and reduce cell death [17]. Therefore,  
244 along with the induction of ferroptosis, the MAPK signaling pathway may be  
245 activated to promote the production of ROS, exacerbate cell damage, and lead to a  
246 vicious cycle.

247 The endogenous apoptotic signaling pathway is the primary biological pathway  
248 involved. Glomerular cell apoptosis is directly related to hemoglobin A1c and systolic  
249 blood pressure, while tubular cell apoptosis is related to the duration of diabetes and

250 low-density lipoprotein cholesterol. Enhanced expression of Fas, Fas ligand, and p38  
251 mitogen-activated protein kinase in glomeruli and tubules suggests that apoptosis may  
252 be a clinically relevant mechanism for the loss of glomerular and tubular cells in type  
253 2 diabetic patients [18]. Diabetic nephropathy is associated with glomerulosclerosis  
254 and impaired renal perfusion. Increasing capillary formation and improving perfusion  
255 may help halt or reverse damage. Transplanting anti-apoptotic p53-silenced  
256 endothelial progenitor cells (p53sh-EPCs) may help improve angiogenesis and renal  
257 perfusion and may be more beneficial than another type of stem cell, such as mouse  
258 mesenchymal stromal cells (mMSCs) [19]. Therefore, the apoptotic signaling  
259 pathway may play a crucial role in ferroptosis after DN.

260 In our study, we identified a crucial module containing two downregulated genes  
261 (MAPK8 and DDIT3) and three upregulated genes (XBP1, HSPA5, and ASNS) using  
262 MCODE. Furthermore, we conducted gene-miRNA analysis on these genes using  
263 miRWalk 2.0 software. Based on our findings, we hypothesize that the ferroptosis-  
264 related key genes MAPK8, has-miR-4775, HSPA5, has-miR-4712-5p/has-miR-770-  
265 5p, and XBP1 interact to form a regulatory network, thereby participating in the  
266 initiation and progression of diabetic nephropathy (DN). Previous studies have shown  
267 that myriocin, an active component of *Cordyceps sinensis*, may exert effects on DN  
268 through various targets such as MAPK8 and TP53, which could facilitate the  
269 development of innovative therapeutic drugs for DN [20]. Immunohistochemical  
270 analysis of renal biopsy samples from DN patients confirmed the upregulation of  
271 HSPA5 protein in renal tubular epithelial cells. These cells undergo endoplasmic  
272 reticulum (ER) stress, and HSPA5 may induce an adaptive and protective unfolded  
273 protein response. While this can protect cells from ER stress, the persistent presence  
274 of hyperglycemia and proteinuria may ultimately lead to apoptosis [21]. Wang et al.  
275 [22] also demonstrated that XBP1 inhibits glomerular mesangial cell apoptosis in  
276 response to oxidative stress through the PTEN/AKT pathway in DN. Madhusudhan  
277 [23] proposed that signaling through the insulin receptor, p85, and XBP1 maintains  
278 podocyte homeostasis, and disruption of this pathway impairs podocyte function in

279 DN. miRNAs are endogenous non-coding RNA molecules that target the 3'UTR  
280 region of genes, regulating gene expression by degrading or inhibiting the translation  
281 of target genes [24]. In our study, we ultimately identified miR-4775, miR-4712-5p,  
282 and miR-770-5p as potentially relevant miRNAs. Therefore, the hypothesis derived  
283 from our data analysis, suggesting that the ferroptosis-related key genes MAPK8, has-  
284 miR-4775, HSPA5, has-miR-4712-5p/has-miR-770-5p, and XBP1 form a regulatory  
285 network involved in the initiation and progression of DN, holds a certain degree of  
286 reliability. This provides important insights for our future fundamental research and  
287 validation efforts, and also suggests a potential target for the development of  
288 therapeutic strategies for DN.

289 The current research has identified several genes closely associated with ferroptosis in  
290 the pathogenesis of DN, some of which have not been previously mentioned in the  
291 context of DN. These novel genes offer new perspectives on ferroptosis in DN and  
292 may provide new therapeutic targets for this process. The identification of these genes  
293 suggests that the regulatory network of MAPK8 molecules may be involved in the  
294 pathogenesis of DN-related ferroptosis.

## 295 **Conclusion**

296 In summary, this study employed bioinformatics analysis to identify potential  
297 ferroptosis-related key genes in the pathogenesis of diabetic nephropathy, thereby  
298 providing new targets for the treatment of DN. The ferroptosis-related key genes  
299 MAPK8, has-miR-4775, HSPA5, has-miR-4712-5p/has-miR-770-5p, and XBP1  
300 interact to form a regulatory network that participates in the initiation and progression  
301 of DN. This provides important references for our future fundamental research  
302 validation efforts and suggests a potential target for the development of therapeutic  
303 strategies for DN.

304

305

306

307

308 **Declaration**

309 **Ethics approval and consent to participate**

310 Not applicable

311 **Consent for publication**

312 Not applicable

313 **Availability of data and material**

314 The datasets generated and/or analyzed during the current study are available in the  
315 [GSE30529] repository, [[https://www.ncbi.nlm.nih.gov/geo/query/acc.cgi?acc=  
316 GSE30529](https://www.ncbi.nlm.nih.gov/geo/query/acc.cgi?acc=GSE30529)].

317 **Competing interests**

318 The authors declare that they have no known competing financial interests or personal  
319 relationships that could have appeared to influence the work reported in this paper.

320 **Funding**

321 The authors declare that they received no funding.

322 **Authors' contribution**

323 All authors contributed to this present work: [SQZ] and [FZ] designed the study.  
324 [SQZ] and [FZ] collected and analyzed data. [SQZ] and [FZ] drafted the manuscript.  
325 [SQZ] and [FZ] reviewed and revised the manuscript. The manuscript has been  
326 approved by all authors for publication.

327 **Acknowledgement**

328 None

329 **Abbreviation**

330 DN, Diabetic Nephropathy

331 ROS, Reactive Oxygen Species

332 iNOS, inducible nitric oxide synthase  
333 Slc7a11, Solute Carrier Family 7 Member 11  
334 MAPK, Mitogen-Activated Protein Kinase  
335 DEGs, Differentially Expressed Genes  
336 DGE, Differential Gene Expression  
337 GSEA, Gene Set Enrichment Analysis  
338 KEGG, Kyoto Encyclopedia of Genes and Genomes  
339 PPIs, Protein-Protein Interactions  
340 MCODE, Molecular Complex Detection  
341 miRNAs, microRNAs  
342 ERK, Extracellular signal-Regulated Kinase  
343 p38 MAPK, p38 Mitogen-Activated Protein Kinase  
344 PTEN, Phosphatase and Tensin Homolog  
345 AKT, AKT Serine/Threonine Kinase  
346 ER, Endoplasmic Reticulum  
347 GSE, Gene Expression Omnibus Series  
348 FDR, False Discovery Rate  
349 DAVID, Database for Annotation, Visualization and Integrated Discovery

350

## 351 **Reference**

- 352 [1] Hong Y, Wang J, Zhang L, Sun W, Xu X, Zhang K. Plasma miR-193a-3p can be a  
353 potential biomarker for the diagnosis of diabetic nephropathy. *Ann Clin Biochem.*  
354 2021; 58: 141-8. doi: 10.1177/0004563220983851.
- 355 [2] Thomas MC, Cooper ME, Zimmet P. Changing epidemiology of type 2 diabetes  
356 mellitus and associated chronic kidney disease. *Nat Rev Nephrol.* 2016; 12: 73-81.  
357 doi: 10.1038/nrneph.2015.173.
- 358 [3] Ning J, Xiang Z, Xiong C, Zhou Q, Wang X, Zou H. Alpha1-Antitrypsin in  
359 Urinary Extracellular Vesicles: A Potential Biomarker of Diabetic Kidney Disease  
360 Prior to Microalbuminuria. *Diabetes Metab Syndr Obes.* 2020; 13: 2037-48. doi:  
361 10.2147/DMSO.S250347.
- 362 [4] Lysaght MJ. Maintenance dialysis population dynamics: current trends and long-  
363 term implications. *J Am Soc Nephrol.* 2002; 13 Suppl 1: S37-40.
- 364 [5] Selby NM, Taal MW. An updated overview of diabetic nephropathy: Diagnosis,  
365 prognosis, treatment goals and latest guidelines. *Diabetes Obes Metab.* 2020; 22

366 Suppl 1: 3-15. doi: 10.1111/dom.14007.

367 [6] Wang Y, Bi R, Quan F, Cao Q, Lin Y, Yue C, Cui X, Yang H, Gao X, Zhang D.  
368 Ferroptosis involves in renal tubular cell death in diabetic nephropathy. *Eur J*  
369 *Pharmacol.* 2020; 888: 173574. doi: 10.1016/j.ejphar.2020.173574.

370 [7] Wu WH, Zhang MP, Zhang F, Liu F, Hu ZX, Hu QD, Yan XY, Huang SM. The  
371 role of programmed cell death in streptozotocin-induced early diabetic nephropathy. *J*  
372 *Endocrinol Invest.* 2011; 34: e296-301. doi: 10.3275/7741.

373 [8] Dixon SJ, Lemberg KM, Lamprecht MR, Skouta R, Zaitsev EM, Gleason CE,  
374 Patel DN, Bauer AJ, Cantley AM, Yang WS, Morrison B, 3rd, Stockwell BR.  
375 Ferroptosis: an iron-dependent form of nonapoptotic cell death. *Cell.* 2012; 149:  
376 1060-72. doi: 10.1016/j.cell.2012.03.042.

377 [9] Qu W, Cheng Y, Peng W, Wu Y, Rui T, Luo C, Zhang J. Targeting iNOS Alleviates  
378 Early Brain Injury After Experimental Subarachnoid Hemorrhage via Promoting  
379 Ferroptosis of M1 Microglia and Reducing Neuroinflammation. *Mol Neurobiol.* 2022;  
380 59: 3124-39. doi: 10.1007/s12035-022-02788-5.

381 [10] Fang X, Cai Z, Wang H, Han D, Cheng Q, Zhang P, Gao F, Yu Y, Song Z, Wu Q,  
382 An P, Huang S, Pan J, et al. Loss of Cardiac Ferritin H Facilitates Cardiomyopathy via  
383 Slc7a11-Mediated Ferroptosis. *Circ Res.* 2020; 127: 486-501. doi:  
384 10.1161/CIRCRESAHA.120.316509.

385 [11] Bao WD, Pang P, Zhou XT, Hu F, Xiong W, Chen K, Wang J, Wang F, Xie D, Hu  
386 YZ, Han ZT, Zhang HH, Wang WX, et al. Loss of ferroportin induces memory  
387 impairment by promoting ferroptosis in Alzheimer's disease. *Cell Death Differ.* 2021;  
388 28: 1548-62. doi: 10.1038/s41418-020-00685-9.

389 [12] Zhou N, Bao J. FerrDb: a manually curated resource for regulators and markers  
390 of ferroptosis and ferroptosis-disease associations. *Database (Oxford).* 2020; 2020.  
391 doi: 10.1093/database/baaa021.

392 [13] Barrett T, Wilhite SE, Ledoux P, Evangelista C, Kim IF, Tomashevsky M,  
393 Marshall KA, Phillippy KH, Sherman PM, Holko M, Yefanov A, Lee H, Zhang N, et  
394 al. NCBI GEO: archive for functional genomics data sets--update. *Nucleic Acids Res.*  
395 2013; 41: D991-5. doi: 10.1093/nar/gks1193.

396 [14] Li S, Huang Y. Ferroptosis: an iron-dependent cell death form linking  
397 metabolism, diseases, immune cell and targeted therapy. *Clin Transl Oncol.* 2022; 24:  
398 1-12. doi: 10.1007/s12094-021-02669-8.

399 [15] Shao X, Zhang X, Hu J, Gao T, Chen J, Xu C, Wei C. Dopamine 1 receptor  
400 activation protects mouse diabetic podocytes injury via regulating the PKA/NOX-  
401 5/p38 MAPK axis. *Exp Cell Res.* 2020; 388: 111849. doi:  
402 10.1016/j.yexcr.2020.111849.

403 [16] Jiang M, Zhang H, Zhai L, Ye B, Cheng Y, Zhai C. ALA/LA ameliorates glucose  
404 toxicity on HK-2 cells by attenuating oxidative stress and apoptosis through the  
405 ROS/p38/TGF-beta1 pathway. *Lipids Health Dis.* 2017; 16: 216. doi:  
406 10.1186/s12944-017-0611-6.

407 [17] Su L, Jiang X, Yang C, Zhang J, Chen B, Li Y, Yao S, Xie Q, Gomez H, Murugan  
408 R, Peng Z. Pannexin 1 mediates ferroptosis that contributes to renal  
409 ischemia/reperfusion injury. *J Biol Chem.* 2019; 294: 19395-404. doi:

410 10.1074/jbc.RA119.010949.  
411 [18] Verzola D, Gandolfo MT, Ferrario F, Rastaldi MP, Villaggio B, Gianiorio F,  
412 Giannoni M, Rimoldi L, Lauria F, Miji M, Deferrari G, Garibotto G. Apoptosis in the  
413 kidneys of patients with type II diabetic nephropathy. *Kidney Int.* 2007; 72: 1262-72.  
414 doi: 10.1038/sj.ki.5002531.  
415 [19] Kundu N, Nandula SR, Asico LD, Fakhri M, Banerjee J, Jose PA, Sen S.  
416 Transplantation of Apoptosis-Resistant Endothelial Progenitor Cells Improves Renal  
417 Function in Diabetic Kidney Disease. *J Am Heart Assoc.* 2021; 10: e019365. doi:  
418 10.1161/JAHA.120.019365.  
419 [20] Qian Y, Sun X, Wang X, Yang X, Fan M, Zhong J, Pei Z, Guo J. Mechanism of  
420 Cordyceps Cicadae in Treating Diabetic Nephropathy Based on Network  
421 Pharmacology and Molecular Docking Analysis. *J Diabetes Res.* 2021; 2021:  
422 5477941. doi: 10.1155/2021/5477941.  
423 [21] Lindenmeyer MT, Rastaldi MP, Ikehata M, Neusser MA, Kretzler M, Cohen CD,  
424 Schlondorff D. Proteinuria and hyperglycemia induce endoplasmic reticulum stress. *J*  
425 *Am Soc Nephrol.* 2008; 19: 2225-36. doi: 10.1681/ASN.2007121313.  
426 [22] Wang Y, He Z, Yang Q, Zhou G. XBP1 inhibits mesangial cell apoptosis in  
427 response to oxidative stress via the PTEN/AKT pathway in diabetic nephropathy.  
428 *FEBS Open Bio.* 2019; 9: 1249-58. doi: 10.1002/2211-5463.12655.  
429 [23] Madhusudhan T, Wang H, Dong W, Ghosh S, Bock F, Thangapandi VR, Ranjan  
430 S, Wolter J, Kohli S, Shahzad K, Heidele F, Krueger M, Schwenger V, et al. Defective  
431 podocyte insulin signalling through p85-XBP1 promotes ATF6-dependent  
432 maladaptive ER-stress response in diabetic nephropathy. *Nat Commun.* 2015; 6: 6496.  
433 doi: 10.1038/ncomms7496.  
434 [24] Sun KT, Chen MY, Tu MG, Wang IK, Chang SS, Li CY. MicroRNA-20a  
435 regulates autophagy related protein-ATG16L1 in hypoxia-induced osteoclast  
436 differentiation. *Bone.* 2015; 73: 145-53. doi: 10.1016/j.bone.2014.11.026.  
437